

# Low-temperature growth mechanism of SWNTs networks by buffer layer-assisted MPCVD

W.H. Wang, Y.R. Peng, P.K. Chuang, C.T. Kuo \*

*Department of Materials Science and Engineering, National Chiao Tung University, Hsinchu, Taiwan*

Available online 9 December 2005

## Abstract

We present the microstructures and growth mechanism of networks of single-walled carbon nanotubes (SWNTs) fabricated by buffer layer-assisted microwave plasma chemical vapor deposition (MPCVD) at relatively low temperatures. The morphologies and bonding structures of carbon nanostructures were characterized by field emission scanning electron microscopy (FESEM), high-resolution transmission electron microscopy (HRTEM), and Raman Spectroscopy. Additionally, the surface roughness of buffer layer and its bonding structures with catalyst atom are analyzed by atomic force microscope (AFM) and X-ray photoelectron spectroscopy (XPS), respectively. Analytical results demonstrate that networks of CNTs are formed by bundles or individual SWNTs. We suggest that the formation of SWNTs networks at low temperature may follow the root-growth mechanism. The differences comparing with previous growth mechanism are that the nuclei formation resulted from the rough surface of the buffer layer, and dissolution of carbon in catalyst will be enhanced due to the surface diffusion of the buffer layer. These unique effects from the buffer layer can provide favorable conditions to grow SWNTs at relatively low process temperatures.

© 2005 Elsevier B.V. All rights reserved.

*Keywords:* Single-walled carbon nanotubes (SWNTs); Buffer layer; Networks; Microwave plasma chemical vapor deposition (MPCVD)

## 1. Introduction

Single-walled carbon nanotubes (SWNTs) can be fabricated by using arc-discharge, laser ablation and catalytic methods [1–4], which are high-temperature processes (above 1500 K). However, these methods are incompatible to IC process when SWNTs are introduced in the application of nano-electrical devices. Therefore, the processes for fabricating SWNTs under low synthesis temperatures were widely developed in the past few years. Arcos et al. [5] presented the alumina buffer layer deposited under a catalyst layer can promote the synthesis of SWNTs effectively at 840 °C. Delzeit et al. [6] also obtained a similar result by incorporating alumina buffer layer and multilayered metal catalysts at ~900 °C. Afterwards, Seidel et al. [7] and Zhong et al. [8] have further reduced the synthesizing temperature of SWNTs to ~600 °C. Very recently, Kuo et al. [9] also employed AlON material as buffer layer and successfully fabricated networks of SWNTs at lower process

temperature (~580 °C) by using plasma chemical vapor deposition (MPCVD). These findings indeed provide a potential process for fabricating SWNTs at much lower temperature; however, their growth mechanism is still not studied thoroughly.

Concerning the growth mechanism of SWNTs, Saito et al. [10] presented the vapor–liquid–solid model to explain the formation of SWNTs fabricated by arc-discharge. Subsequently, Gavillet et al. [11] suggested that root-growth mechanism could explain the growth of SWNTs by different techniques because their morphologies are very similar. Nevertheless, the morphologies of buffer layer-assisted SWNTs networks are not exactly same as that fabricated by high-temperature processes (e.g., arc-discharge). Hence, it is a debated issue that root-growth mechanism also can explain the growth of SWNTs networks fabricated by low-temperature processes. In this work, SWNTs networks were fabricated by buffer-layer-assisted Co-catalyst MPCVD and each process step was examined to study the possible growth mechanisms. We present the microstructures very detailed and propose a model to explain growth mechanism of SWNTs networks fabricated at low process temperature.

\* Corresponding author. Tel.: +886 3 5731 949; fax: +886 3 5724727.

E-mail address: [ctkuo@mail.nctu.edu.tw](mailto:ctkuo@mail.nctu.edu.tw) (C.T. Kuo).

## 2. Experimental

Since Kuo et al. have reported the AION film shows strong effects to enhance the SWNTs formation [9], the AION material was employed as the buffer layer in this work. First, AION buffer layer of 10 nm was deposited on the silicon wafer via DC reactive sputtering, and the Co catalyst layer of 5 nm was subsequently deposited. Then, the specimen was followed by H-plasma pretreatment (100 sccm H<sub>2</sub> for 10 min) in MPCVD system to make a Co catalyst film to become well-distributed nanoparticles and subsequently were deposited under CH<sub>4</sub>/H<sub>2</sub> atmospheres (5 sccm/50 sccm) to form networks of SWNTs at ~620 °C, where the process temperature is controlled by a chamber working pressure. The specimen without the buffer layer is performed under the same process condition to make a comparison. The detailed process parameters are described elsewhere [9]. Morphologies of networks of SWNTs were characterized by FESEM and HRTEM and their bonding structures were examined by Raman spectroscopy with a 632.8-nm He–Ne laser. Additionally, the surface roughness, structure of AION film and interaction between Co/AION layer were analyzed by atomic force microscopy (AFM), X-ray diffraction (XRD) and X-ray photoelectron spectroscopy (XPS), respectively.

## 3. Results and discussion

### 3.1. Microstructures of SWNTs networks

Fig. 1 shows the FESEM morphology of as-deposited carbon nanostructures assisted by the buffer layer, where networks of CNTs are linked between the neighboring catalyst nanoparticles. By contrast, there are no CNTs found in the specimen without the buffer layer. To clarify the bonding structure, the Raman spectrum of as-deposited carbon nanostructures is shown in Fig. 2. There are strong peaks of radial breath mode (RBM) and high  $I_G/I_D$  ratio can be found in the Raman spectrum, indicating the existence of a highly graphitized SWNTs [12]. These results indicate that the networks of SWNT are indeed synthesized successfully in this experiment.

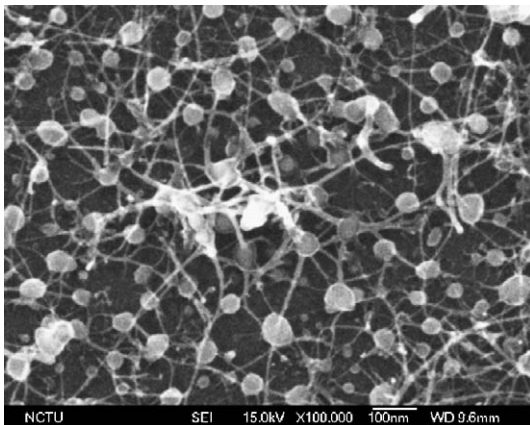


Fig. 1. SEM micrograph of SWNTs networks grown on silicon wafer with AION materials as buffer layers of Co catalyst.

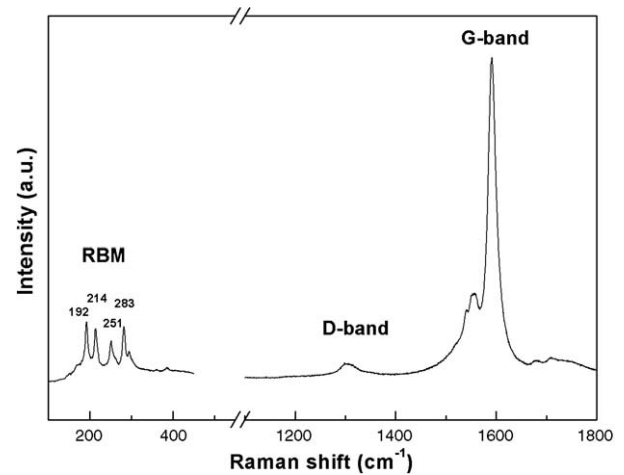


Fig. 2. Raman spectrum of SWNTs networks grown on silicon wafers with AION buffer layer.

The diameter of SWNTs can be estimated by the theoretical calculation from the positions of RBM peaks [13] and predict that their diameters are varied from 0.8 to 1.3 nm.

To investigate their structures directly, the HRTEM images of networks of SWNTs are shown in Fig. 3(a) and (b). It consists of SWNTs with a diameter of 1.1 nm and networks are found to be formed by bundles of SWNTs as shown in Fig. 3(a). The diameters of SWNTs observed in HRTEM image are in agreement with those of calculating in the Raman spectrum. It is interesting to observe some networks are connected by individual SWNTs as depicted in Fig. 3(b). It supports the evidence that nanotubes cannot be found in the FESEM image under some process conditions but still show strong RBM peak in the Raman spectra.

These HRTEM results show the SWNT ropes grown from catalyst particles radially, where their morphologies are similar to those observed by Saito et al. [10,11]. It suggests that the formation of buffer-layer-assisted SWNTs may follow the proposed root-growth mechanism [11]. It is most interesting to note that the suggested Ni catalyst size to grow SWNT ropes following root-growth is ~15 nm in previous research [10,14]. However, these SWNT ropes with network structures can be found to grow from large-sized Co catalyst particles (~50 nm, refer to Fig. 1). It indicates that the critical catalyst size to form SWNT ropes strongly depends on the fabrication methods and catalyst materials. Several metal materials, such as Fe, Ni, and Gd, have been studied as catalysts for fabricating SWNTs successfully and present similar morphologies in the previous study. In this paper, we observe a similar microstructure by using Co metal as the catalyst material under buffer-layer-assisted growth and find that the suggested size of catalyst is quite large.

From the above results, we can observe some interesting phenomenon comparing with previous reports. First, the diameter (0.8–1.3 nm) of SWNTs synthesized in this case is similar with those fabricated by the arc method [10,11]. However, the larger size and wider tube diameter distribution (0.9–3.0 nm) are obtained in Zhong's [8] result, which also employs alumina as the buffer material by using MPCVD at ~600 °C of synthesis temperature. This difference might have

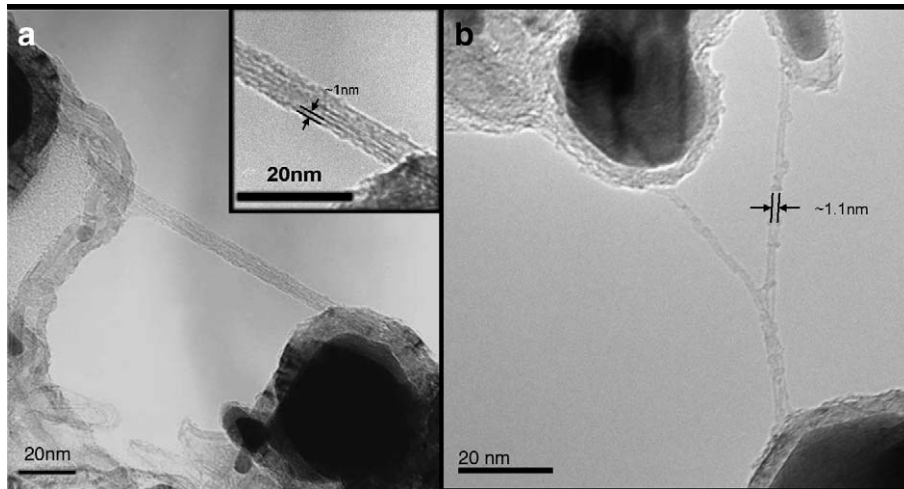


Fig. 3. HRTEM images of SWNTs networks grown on silicon wafers with AlON buffer layer. In (a) the networks are formed by bundles of SWNTs; in (b) networks are formed by individual SWNT.

resulted from the roughness condition of the buffer layer, which will be discussed in the next paragraph. Secondly, the catalyst size is quite large compared with those fabricated by the high-temperature process [10,11] but also for low-temperature methods [8,9,15,16]. Usually, the diameter of SWNT is quite similar as its catalyst size among CVD processes. Therefore, the deposited thickness of catalyst is very thin (<1 nm) in previous researches [11]; by contrast, the catalyst thickness that we deposited is relatively thick (5–10 nm) and still obtain the SWNTs in our experiment. It is concluded that the microstructures and growth conditions might be different even if using the same concept (alumina buffer) or the low-temperature CVD process.

### 3.2. Effects of buffer layer on SWNTs formation

To study the key role played by the buffer layer, the surface structure of the as-deposited AlON film is characterized by X-ray diffraction and AFM, respectively. The X-ray diffraction result shows that the AlON as-deposited film with 10 nm in thickness is in an amorphous state. Fig. 4 displays the

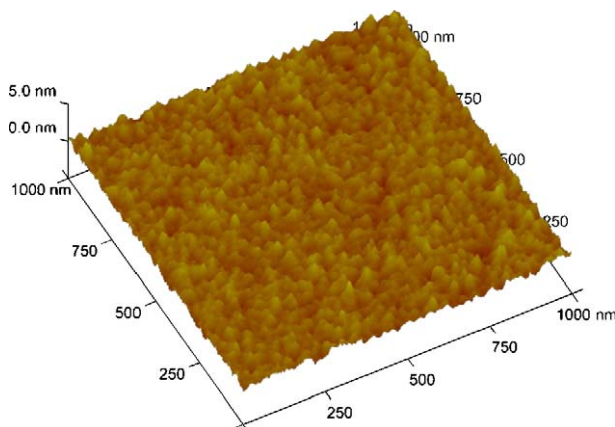


Fig. 4. AFM image of AlON buffer layer of 10 nm shows a rough surface. The rms value of surface roughness is  $\sim 1.0$  nm.

roughness of AlON film is  $\sim 1$  nm, whereas the Si wafer surface is quite neat. We also have measured the roughness of other buffer materials for comparison, such as AlN, TiN, and TiO<sub>2</sub>, which have been studied and show hardly any effect to enhance SWNTs growth in previous reports [7, 9]. The AFM results show that their surface is quite smooth and their roughness ( $R_{\text{rms}}$ ) are on the order of angstroms at most. These results suggest that the protrusion on the rough buffer layer (e.g., AlON) can cause instabilities on the Co catalyst surface and form nuclei sites for tube growth afterwards. This heterogeneous nucleation phenomenon of metal deposited on oxide film has been revealed in past studies [17]. To clarify the effects of the buffer layer with larger roughness, the AlON film of 5 nm ( $R_{\text{rms}}$ ,  $\sim 2.0$  nm) was employed to perform the experiment under the same process condition. The SEM image and Raman spectra results show that the amount of CNTs is very few and only a very weak RBM signal can be detected. Therefore, we conclude that the buffer layer with appropriate roughness value is the favorable condition to form the nuclei on the catalyst for SWNTs growth.

To examine the nanostructures after H-plasma pre-treatment, SEM morphologies of Co catalyst particles on buffer layer and Si wafer are shown in Fig. 5(a) and (b), respectively. It shows that the Co catalyst layer deposited on the AlON buffer layer will become larger particles ( $\sim 60$  nm) than those on the Si wafer ( $\sim 30$  nm). It is believed that the size of the Co catalyst particles after pretreatment is determined by the wetting properties between the substrate and catalyst material. Usually, catalyst particles with small size are considered to possess higher reactivity which is in favor of CNT growth; however, we found that the catalyst size is not the most important factor to affect the growth of SWNTs in this case.

Except the nucleation factor, it is well known that the carbon solubility of the catalyst is also the most important issue. Previous researches [18] reported that alumina-supported transition metals possess higher reactivity for NO reduction by C<sub>3</sub>H<sub>6</sub>. Furthermore, Matolin's group [19–21] also revealed that adsorption and dissociation probability of CO gas on metal

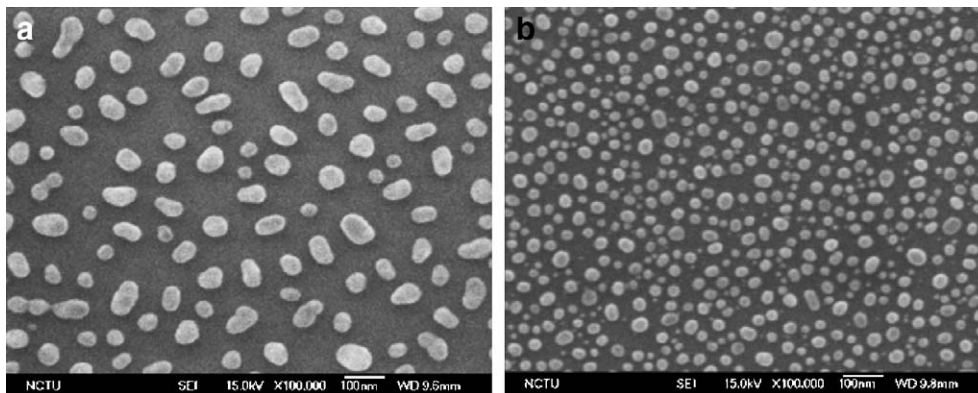


Fig. 5. SEM micrographs of Co catalyst layer after pretreatment on silicon wafers: (a) with AlON buffer layer; (b) without buffer layer.

particles, which deposited on alumina substrate, will be increased due to the surface diffusion effect. These findings indicate that the reaction activity of alumina-supported metal is increased remarkably. It is believed that the extra carbon species that dissociated from the source gas will diffuse into the catalyst particles along the alumina surface and dissolve into the catalyst. This phenomenon will cause the catalyst to possess higher carbon species concentration than those without alumina support (Si substrate) and provide a favorable condition for CNTs growth. It supports a reasonable explanation that SWNTs can grow from a Co catalyst successfully under a quite low temperature in our study.

To clarify whether other compounds (e.g.,  $\text{Co}_3\text{O}_4$ ) participate in this effect, the XPS analysis of carbon nanostructures was performed as shown in Fig. 6. It is found that the Co peak appears at 784 eV and a small shifted value (pure Co peak is at 782 eV) may have resulted from the slightly oxidation due to the sample exposure to the air before analysis. It is expected that the strongest intensity oxygen peak appears at 532 eV from AlON layer which is very close to the peak of  $\text{Al}_2\text{O}_3$  (531.1 eV), indicating the nonexistence of other Co oxides (oxygen will appear at 536.1 eV if  $\text{Co}_3\text{O}_4$  is formed [22]). Furthermore, it is found that the Al peak appears at 75 eV, indicating no other

aluminum compounds forming, such as  $\text{CoAl}_2\text{O}_4$ , where Al peak is 73.6 eV [23–25]. Therefore, we can conclude that there is no compound formation and the effect to enhance SWNTs growth is mainly caused by an alumina buffer layer.

In summary, we suggest that the key factors to enhance the SWNTs formation are the appropriate film roughness of the buffer layer and the high reaction activity of the Co catalyst deposited on the buffer layer. It is concluded that the rough surface of the AlON buffer layer can form numerous nucleation sites on the catalyst surface during the sputtering and pretreatment process. Then, supersaturation carbon will precipitate from these nucleation sites to form SWNTs in the following process. The dissolution concentration of carbon in the catalyst is increased remarkably due to the surface diffusing effect on the AlON substrate and provides enough carbon species for CNTs growth at low temperature.

### 3.3. Growth mechanism

We present a sketch of the proposed scenario in Fig. 7. The first step is that large-sized crystallites are formed after pretreatment which are determined by the wetting properties. The numerous instabilities, which resulted from the protrusions on the rough AlON buffer layer, are formed on the surface of Co catalyst particles as the nuclei for tube growth (Fig. 7b). The second step is the dissolution of carbon and the precipitation of the supersaturation carbon from the catalyst particles (Fig. 7c). Excess carbon species will diffuse into the catalysts along the substrate surface except that the catalyst surface and the supersaturation carbon will precipitate from the nuclei at the lateral zone of Co particles where the temperature is relatively low.

The third stage is the growth process of SWNTs depicted in Fig. 7d. The numerous SWNT ropes are grown and formed as bundles of SWNTs due to van der Waal's forces. There is a competition between the nucleation of SWNTs and the graphitic layers at this stage. It is in agreement with the proposed models by Saito [10] and Gavillet et al. [11] and explains that we can observe some particle-covered graphite layer only and CNTs were not found under some experimental conditions. Saito et al. [11] proposed the rapid cooling rate of catalyst particles, which can promote the nuclei formation, and high supersaturation

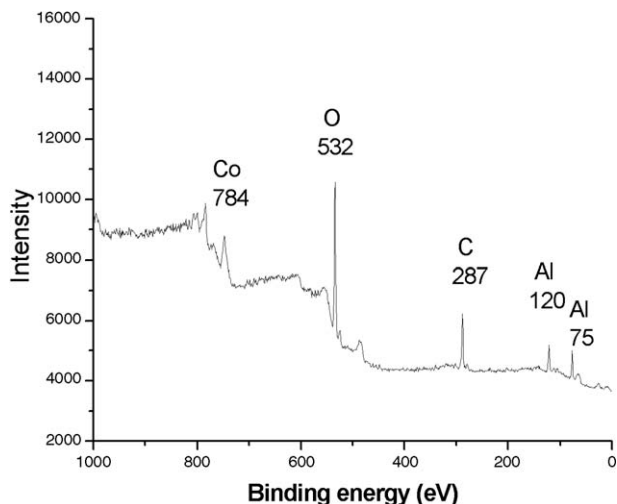


Fig. 6. XPS spectrum of as-deposited carbon nanostructures on silicon wafer with AlON buffer layer.

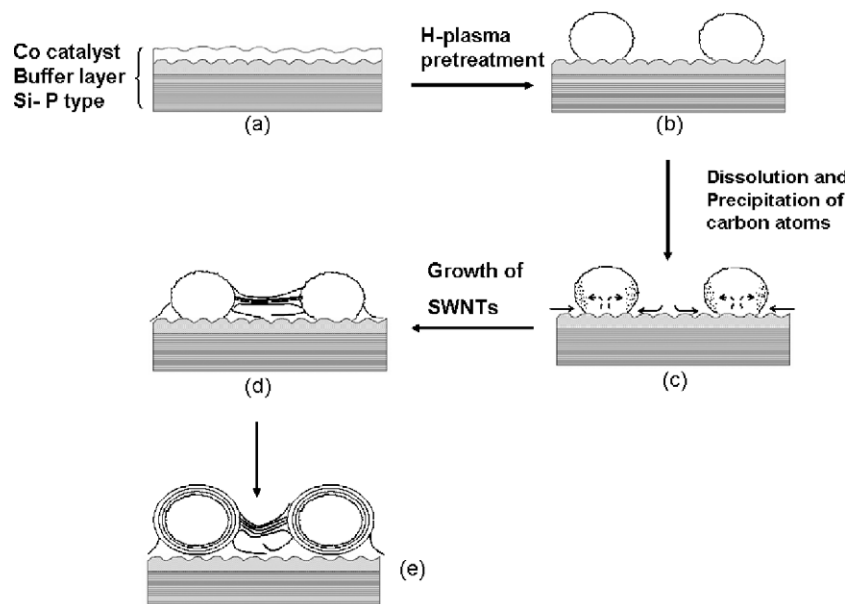


Fig. 7. The hypothetical growth process of SWNTs networks assisted by buffer layer at low temperature by MPCVD.

carbon are the favorable conditions to grow SWNTs. However, the cooling rate in an MPCVD system cannot be achieved in a similar rate as arc-discharge method because our presenting process temperature is only  $\sim 620$  °C. Restated, the formation of the nuclei on the catalyst surface is not dominated by the cooling rate but other factors. Therefore, we propose that these nuclei for SWNTs growth are mainly enhanced by a thin amorphous AlON buffer layer, which provides an appropriate rough surface. Finally, when the growth time is long enough, a few layers of graphitic layers will be formed and force SWNT ropes to depart from the catalyst (Fig. 7e).

It is concluded that networks of SWNTs fabricated by buffer-layer-assisted Co catalyst-MPCVD at low temperature may follow root-growth mechanism but its nucleation mechanism and enhancement of catalyst activity for carbon dissolution are quite different compared with previous report.

#### 4. Conclusions

Microstructures and possible growth mechanism of buffer-layer-assisted SWNTs networks fabricated by MPCVD at low temperature are investigated. The HRTEM images show networks are formed as ropes of SWNTs or individual SWNTs. We present a similar root-growth model to explain its growth mechanism. First, numerous nuclei for SWNTs growth are formed on the Co particle surface due to the protrusions of a thin and rough buffer layer surface. Then, dissociation carbon species will dissolve into Co nano-particles from their surface and along the buffer layer surface when carbon source gases are introduced. Subsequently, the supersaturation carbon will precipitate from the nucleation sites, which occurs once conquering the competition of graphitic layers, located at lateral side of the catalyst particles. Finally, SWNTs are grown from the catalyst particles to form a network morphology between neighboring particles. Afterwards, the excess carbon

species will precipitate constantly to form graphitic layers and force the SWNTs rope to depart from the catalyst.

#### Acknowledgments

This work was supported in part by the National Science Council of Taiwan, under Contract No. NSC93-2216-E-009-004, NSC93-2216-E-009-009, and NSC93-2120-M-009-003.

#### References

- [1] C. Journet, W.K. Maser, P. Bernier, A. Loiseau, M. Lamy de la Chapelle, S. Lefrant, P. Deniard, R. Lee, J.E. Fischer, *Nature* 388 (1997) 756.
- [2] A. Thess, R. Lee, P. Nikolaev, H. Dai, P. Petit, J. Robert, C. Xu, Y.H. Lee, S.G. Kim, A.G. Rinzler, D.T. Colbert, G.E. Scuseria, D. Tomaacutenek, J.E. Fischer, R.E. Smalley, *Science* 273 (1996) 483.
- [3] H.M. Cheng, F. Li, G. Su, H.Y. Pan, L.L. He, X. Sun, M.S. Dresselhaus, *Appl. Phys. Lett.* 72 (1998) 3282.
- [4] J.F. Colomer, L. Henrard, G. van Tendeloo, A. Lucas, P. Lambin, *Chem. Commun.* 14 (1999) 1343.
- [5] T. de los Arcos, M.G. Garnier, P. Oelhafen, D. Mathys, J.W. Seo, C. Domingo, J.V. Garcia-Ramos, S. Sanchez-Cortes, H.J. Dai, J.H. Hafner, A.G. Rinzler, D.T. Colbert, *Carbon* 42 (2004) 187.
- [6] L. Delzeit, B. Chen, A. Cassell, R. Stevens, C. Nguyen, M. Meyyappan, *Chem. Phys. Lett.* 348 (2001) 368.
- [7] R. Seidel, G.S. Duesberg, E. Unger, A.P. Graham, M. Liebau, F. Kreupl, *J. Phys. Chem.* 108 (2004) 1888.
- [8] G. Zhong, T. Iwasaki, K. Honda, Y. Furukawa, I. Ohdomari, H. Kawarada, *Jpn. J. Appl. Phys.* 44 (2005) 1558.
- [9] W.H. Wang, Y.R. Peng, B.K. Chuang, C.T. Kuo, *Diamond Relat. Mater.*, in press.
- [10] Y. Saito, M. Okuda, N. Fujimoto, T. Yoshikawa, M. Tomita, T. Hayashi, *Jpn. J. Appl. Phys.* 33 (1994) 526.
- [11] J. Gavillet, C. Journet, F. Willaime, F. Ducastelle, J.-C. Charlier, *Phys. Rev. Lett.* 87 (2001) 275504.
- [12] A.M. Rao, E. Richter, S. Bandow, *Science* 275 (1997) 187.
- [13] A. Jorio, G. Souza, G. Dresselhaus, M.S. Dresselhaus, A.K. Swan, M.S. Unlu, B.B. Goldberg, M.A. Pimenta, J.H. Hafner, C.M. Lieber, R. Saito, *Phys. Rev.*, B 65 (2002) 155412.

- [14] D. Zhou, S. Seraphin, S. Wang, *Appl. Phys. Lett.* 65 (1994) 1593.
- [15] Y. Li, D. Mann, M. Rolandi, W. Kim, A. Ural, S. Hung, A. Javey, J. Cao, D. Wang, E. Yenilmez, Q. Wang, J.F. Gibbons, Y. Nishi, H. Dai, *Nano Lett.* 4 (2004) 317.
- [16] H. Liao, J.H. Hafner, *J. Phys. Chem., B* 108 (2004) 6941.
- [17] M. Baumer, H.-J. Freund, *Prog. Surf. Sci.* 61 (1999) 127.
- [18] T.W. Kim, M.W. Song, H.L. Koh, K.L. Kim, *Appl. Catal.* 210 (2001) 35.
- [19] I. Stara, V. Nehasil, V. Matolin, *Surf. Sci.* 365 (1996) 69.
- [20] V. Nehasil, I. Stara, V. Matolin, *Surf. Sci.* 377–379 (1997) 813.
- [21] I. Jungwirthova, I. Stara, V. Matolin, *Surf. Sci.* 377–379 (1997) 644.
- [22] S. Ram, D. Ghosh, S.K. Roy, *J. Mater. Sci.* 36 (2001) 3745.
- [23] T.A. Patterson, J.C. Carver, D.E. Leyden, D.M. Hercules, *J. Phys. Chem.* 80 (1976) 1702.
- [24] V.I. Nefedov, *J. Electron Spectrosc. Relat. Phenom.* 25 (1982) 29.
- [25] C.D. Wagner, J.A. Taylor, *J. Electron Spectrosc. Relat. Phenom.* 20 (1980) 83.